Published in final edited form as:
Bioconjug Chem. 2008 July ; 19(7): 1439–1447.

Novel Bimodal Bifunctional Ligands for Radioimmunotherapy and Targeted MRI

Hyun-Soon Chong[1,*], **Hyun A Song**[1], **Xiang Ma**[1], **Diane Milenic**[2], **Erik Brady**[2], **Sooyoun Lim**[1], **Haisung Lee**[1], **Kewamena Baidoo**[2], **Dengfeng Cheng**[1], and **Martin W Brechbiel**[2]

1*Chemistry Division, Biological, Chemical, and Physical Sciences Department, Illinois Institute of Technology, Chicago, IL.*

2*Radioimmune & Inorganic Chemistry Section, Radiation Oncology Branch, Center for Cancer Research, National Cancer Institute, NIH, Bethesda, MD.*

Abstract

The structurally novel bifunctional ligands *C*-NETA and *C*-NE3TA, each possessing both acyclic and macrocyclic moieties, were prepared and evaluated as potential chelates for radioimmunotherapy (RIT) and targeted magnetic resonance imaging (MRI). Heptadentate *C*-NE3TA was fortuitously discovered during the preparation of *C*-NETA. An optimized synthetic method to *C*-NETA and *C*-NE3TA including purification of the polar and tailing reaction intermediates, *tert*-butyl *C*-NETA (2) and *tert*-butyl *C*-NE3TA (3) using semi-prep HPLC was developed. The new Gd(III) complexes of *C*-NETA and *C*-NE3TA were prepared as contrast enhancement agents for use in targeted MRI. The T1 Relaxivity data indicates that Gd(*C*-NETA) and Gd(*C*-NE3TA) possess higher relaxivity than Gd(*C*-DOTA), a bifunctional version of a commercially available MRI contrast agent, Gd(DOTA). *C*-NETA and *C*-NE3TA were radiolabeled with ^{177}Lu, ^{90}Y, ^{203}Pb, $^{205/6}$Bi and ^{153}Gd, and *in vitro* stability of the radiolabeled corresponding complexes was assessed in human serum. The *in vitro* studies indicate that the evaluated radiolabeled complexes were stable in serum for 11 days with the exception being the ^{203}Pb complexes of *C*-NETA and *C*-NE3TA which dissociated in serum. *C*-NETA and *C*-NE3TA radiolabeled ^{177}Lu, ^{90}Y, or ^{153}Gd complexes were further evaluated for *in vivo* stability in athymic mice and possess excellent or acceptable *in vivo* biodistribution profile. $^{205/6}$Bi-*C*-NE3TA exhibited extremely rapid blood clearance and low radioactivity level at the normal organs, while $^{205/6}$Bi-*C*-NETA displayed low radioactivity level in the blood and all of the organs except for the kidney where relatively high renal uptake of radioactivity is observed. *C*-NETA and *C*-NE3TA were further modified for conjugation to the monoclonal antibody Trastuzumab.

Introduction

Radioimmunotherapy (RIT) (1) and magnetic resonance imaging (MRI) (2) are promising techniques for targeted treatment or imaging of numerous cancer types. Both modalities require the use of either radioactive or non-radioactive metals, either of which can be very toxic when deposited in normal tissues *in vivo*, causing life-threatening side effects (3). Therefore, the success of clinical applications of both RIT and MRI depends heavily on the performance of the metal-binding ligands. RIT employs a monoclonal antibody (mAb) for selective delivery

*To whom correspondence should be addressed. E–mail: Chong@iit.edu, Phone: 312-567-3235, Fax: 312-567-3494. Mailing address: 3101 S. Dearborn St, LS 182, Illinois Institute of Technology, Chemistry Division, Biological, Chemical, and Physical Science Department, Chicago, IL, 60616.

Supporting Information Available: Relaxivity data of Gd(*C*-NETA), Gd(*C*-NE3TA), and Gd(*C*-DOTA). This material is available free of charge via the Internet at http://pubs.acs.org/BC.

of a cytotoxic radionuclide to tumor cells while minimizing toxicity due to non-selective exposure of the radionuclide to the normal healthy cells (4,5). The RIT scenario requires three components: a radionuclide, a mAb, and a bifunctional ligand (6). The first RIT drug, Zevalin® consists of an anti-CD20 antibody, 1B4M-DTPA (2-(4-nitrobenzyl)-6-methyl-diethylenetriaminepentaacetic acid), and ^{90}Y, and has proven to have significant potency against B-cell non-Hodgkin's lymphoma (7,8). The radionuclides ^{177}Lu, ^{90}Y, ^{212}Pb, ^{212}Bi, and ^{213}Bi are all recognized as promising metallic radionuclides for effective RIT (5,6). An effective bifunctional ligand conjugated to a sensitive mAb that can rapidly form a stable complex with a short-lived radionuclide must be employed to minimize toxicity due to either dissociation of metal complex or radiolytic damage resulting from extended exposure of the protein during radiolabeling (9-11). Although numerous RIT using the radioisotopes have been explored to treatment of various cancers, less progress has been made on development of new bifunctional ligands that might address limitations of the currently available bifucntional ligands, *C*-DOTA (2-(4-nitrobenzyl)-1,4,7,10-tetraazacyclododecane tetraacetic acid) and *C*-DTPA (2-(4-nitrobenzyl)-diethylenetriamine pentaacetic acid), that are related to slow complexation kinetics and low complex stability, respectively (12).

MRI is a powerful diagnostic medical tool that provides non-invasive and high resolution imaging for a variety of applications(2,13). MRI gives distribution of the MR signal intensity resulting from the longitudinal (T_1) and the transverse (T_2) magnetic relaxation times of water protons. Images with a clear contrast between tissues with different relaxation times of water protons can be obtained with MRI (2). The lanthanide Gd(III) is known to be an optimal paramagnetic metal for MRI due to high electronic spin (7/2) and slow electronic relaxation rate (14). Stable Gd(III) complexes with low toxicity and efficient excretion profiles are required for *in vivo* use since free Gd(III) is toxic causing severe side effects (15). A number of Gd(III) complexes such as Gd(DOTA) and Gd(DTPA) are clinically approved for use in MRI (2). However, most contrast agents have non-specific extracellular distribution and with the disadvantages of low relaxivity, low tissue specificity, and rapid clearance. Considerable research efforts have been directed towards developing safe Gd(III)-based MR contrast agents with high tissue specificity and sensitivity. Development of bifunctional ligands with a functional unit for conjugation to a targeting moiety that can tightly sequester Gd(III) is required for targeted MRI with high sensitivity and specificity.

Previously, we reported that NETA to be a promising chelate for RIT and MRI applications (16-18). The bimodal ligand NETA ({4-[2-(Bis-carboxymethyl-amino)-ethyl]-7-carboxymethyl-[1,4,7]triazonan-1-yl}-acetic acid) possesses a parent macrocyclic ligand and a flexible acyclic multidentate pendant arm and is designed to integrate the advantages of the macrocyclic DOTA (1,4,7,10-tetraazacyclododecane-tetraacetic acid) and acyclic DTPA (diethylenetriaminepenta acetic acid) frameworks and with this hybridization to provide high thermodynamic stability and favorable formation kinetics for complexation of metal ions of interest. Indeed, non-functionalized NETA displayed significantly enhanced complexation kinetics with Y(III) (16), Lu(III) (19), and Bi(III) (19) as compared to DOTA. The NETA complexes radiolabeled with ^{90}Y (16), ^{177}Lu (17), or ^{153}Gd (18) exhibited excellent *in vitro* serum stability and demonstrated excellent or acceptable *in vivo* biodistribution profiles. NETA was also evaluated as the chelate of Gd(III) for MRI. NETA-Gd(III) complex displayed enhanced relaxivity comparable to that of DOTA-Gd(III) (18). NETA radiolabeled with ^{153}Gd was exceptionally stable in serum and mice (18). With the proven potential of NETA for RIT and MRI, we have moved forwards with synthesis of a bifunctional version of NETA and NETA analogue possessing a linker for conjugation to a targeting moiety for RIT and for targeted MRI. In this paper, we describe the synthesis and evaluation of a bifunctional version of NETA, *C*-NETA ({4-[2-(Bis-carboxymethyl-amino)-3-(4-nitro-phenyl)-propyl]-7-carboxymethyl[1,4,7]tri-azonan-1-yl}-acetic acid) and its heptadentate analogue *C*-NE3TA

({4-carboxymethyl-7-[2-(carboxymethyl-amino)-3-(4-nitro-phenyl)-propyl]-[1,4,7]triazo-nan-1-yl}-acetic acid) for RIT and MRI.

Experimental Procedures

Instruments and methods

^{1}H and ^{13}C NMR spectra were obtained using a Bruker 300 instrument and chemical shifts are reported in ppm on the δ scale relative to TMS, TSP, or solvent. Elemental microanalyses were performed by Galbraith Laboratories, Knoxville, TN. Fast atom bombardment (FAB) high resolution mass spectra (HRMS) were obtained on JEOL double sector JMS-AX505HA mass spectrometer (University of Notre Dame, IN). Analytical HPLC was performed on Agilent 1200 (Agilent, Santa Clara, CA) equipped with a dioarray detector (λ = 254 and 280 nm), themostat set at 35 °C and a Zorbax Eclipse XDB-C18 column (4.6 × 150 mm, 80Å, Agilent, Santa Clara, CA). The mobile phase of a binary gradient (0-100%B/40 min; solvent A = 0.05 M AcOH/Et_3N, pH 6.0; solvent B = CH_3CN for method 1 or solvent A = 0.05 M AcOH/Et_3N, pH 6.0; solvent B = CH_3OH for method 2; (0-50%B/30 min solvent A = 0.05 M AcOH/Et_3N, pH 6.0; solvent B = CH_3OH for method 5) or a binary gradient and isocratic (0-100% B/40 min and 100%B/40-50min; solvent A = 0.05 M AcOH/Et_3N, pH 6.0; solvent B = CH_3CN for method 6) at a flow rate of 1 mL/min was used. Semi-prep HPLC was performed on an Agilent 1200 equipped with a dioarray detector (λ = 254 and 280 nm), themostat set at 35 °C, and a Zorbax Eclipse XDB-C18 column (9.4 × 250 mm, 80Å). The mobile phase of a binary gradient (0-100%B/160 min; solvent A = 0.05 M AcOH/Et_3N, pH 6.0; solvent B = CH_3CN for method 3 or 0-50%B/30 min, solvent A = H_2O, pH 6.0; solvent B = methanol for method 4) at a flow rate of 3 mL/min was used. Size exclusion HPLC (SE-HPLC) chromatograms were obtained on a Lab Alliance isocratic system (model: QGrad, State College, PA) with a Waters 717plus autosampler (Milford, MA), a Gilson 112 UV detector (Middleton, WI) and an in-line IN/US γ-Ram Model 2 radiodetector (Tampa, FL), fitted with a TSK G3000PW column (Tosoh Biosep, Montgomeryville, PA).

Reagents

All reagents were purchased from Sigma-Aldrich (St. Louis, MO) and used as received unless otherwise noted. Phosphate buffered saline (PBS), 1X, pH 7.4 consisted of 0.08 M Na_2HPO_4, 0.02 M KH_2PO_4, 0.01 M KCl, and 0.14 M NaCl. ^{90}Y in the chloride form was purchased from Perkin Elmer Life Sciences (Shelton, CT). ^{177}Lu in the chloride form was obtained from NEN Perkin-Elmer. ^{86}Y, $^{205,6}Bi$, and ^{203}Pb were produced using a CS30 cyclotron (PET Dept, Clinical Center, NIH) and purified as described previously (17,18). C-DOTA was purchased from Macrocyclics (Dallas, TX). ^{153}Gd was obtained from Isotope products (Valencia, CA). ^{157}Gd and ^{115}In were obtained from Sigma-Aldrich (St. Louis, MO)

Tert-butyl {4-*tert*-Butoxycarbonylmethyl-7-[2-(*tert*-butoxycarbonylmethyl-amino)-3-(4-nitro-phenyl)-propyl]-[1,4,7]triazonan-1-yl}-acetic acetate (3)

To a slurry of **1** (26) as an acidic salt (2.27 g, 5 mmol) in DMF (50 mL) at 0 °C was added DIPEA (6.5 g, 50.25 mmol), KI (996 mg, 6mmol). *Tert*-butyl bromoacetate (3.22 g, 16.5 mmol) was added drop wise over 20 min. The resulting mixture was stirred for 2 h at 0 °C and for 2 h at room temperature. The reaction mixture was heated to 50 °C and stirred for 19 h after which time the reaction mixture was cooled to room temperature and then to 0 °C. 6 M HCl (3.5 mL) and heptane (30 mL) were sequentially added to the solution. The resulting solution was vigorously stirred for 5 min, and the heptane layer was separated. The aqueous layer was extracted with heptane (2 × 30mL), and treated with 10% Na_2CO_3 (45 mL). Additional heptane (30 mL) was added into the aqueous solution, and the resulting mixture was stirred for 30 min, and the heptane layer was separated. The combined heptane layers were washed with water (10 mL), dried ($MgSO_4$), filtered, and concentrated *in vacuo*. The residue was on silica gel

(220-400 mesh) column eluted with 20%-30% CH_3OH/CH_2Cl_2 and 0.5 mL Et_3N in 20%-30% CH_3OH/CH_2Cl starting from CH_2Cl_2 to provide pure **3** (2.21 g, 68%): ^{1}H NMR ($CDCl_3$) δ 1.41 (s, 27 H), 2.30-2.52 (m, 3 H), 2.63-2.94 (m, 16 H), 3.20-3.36 (m, 6 H), 7.36 (d, J = 8.01 Hz, 2 H), 8.15 (d, J = 8.01 Hz, 2 H); ^{13}C NMR ($CDCl_3$) δ 28.98, 28.09, 39.32, 49.83, 55.84, 56.04, 56.92, 59.48, 62.62, 80.36, 80.76, 123.32, 130.11, 146.36, 147.47, 171.07, 171.40; HRMS (Positive ion FAB) Calcd for $C_{33}H_{56}N_5O_8$ $[M + H]^+$ *m/z* 650.4129. Found: $[M + H]^+$ *m/z* 650.4110. Analytical HPLC (t_R = 32.6 min, method 6). Isolation of **3** from the reaction mixture was achieved using semi-HPLC (method 3). The mixture was dissolved in 1 mL of CH_3OH, and the fractions from 79 – 101 min was collected, evaporated, dissolved in CH_2Cl_2, and washed with H_2O. The organic layer was dried, filtered, evaporated, and concentrated *in vacuo* to afford the desired **3**.

{4-Carboxymethyl-7-[2-(carboxymethyl-amino)-3-(4-nitro-phenyl)-propyl]-[1,4,7]triazonan-1-yl}-acetic acid (*C*-NE3TA)

Compound **3** (60 mg, 0.09 mmol) was treated with 4M HCl in 1, 4-dioxane (5 mL) at 0 °C. The resulting mixture was gradually warmed to room temperature and stirred for 18 h. Diethyl ether (100 mL) was added into the reaction mixture, and the resulting mixture was placed in the freezer for 2 h. The precipitate was filtered, immediately dissolved in water (10 mL), and washed with diethyl ether (20 mL). The aqueous layer was lyophilized to provide pure *C*-NE3TA as a light brownish solid (54 mg, 95%): ^{1}H NMR (D_2O) δ 2.42-2.60 (m, 1 H), 2.80-3.39 (m, 14 H), 3.68-3.92 (m, 8 H), 7.45 (d, *J* = 7.9 Hz, 2 H), 8.16 (d, *J* = 7.9 Hz, 2 H); ^{13}C NMR (D_2O) δ 36.6, 47.5, 51.4, 52.3, 54.3, 58.6, 61.1, 126.8, 132.9, 145.7, 149.6, 171.6, 174.0. HRMS (Positive ion FAB) Calcd for $C_{21}H_{32}N_5O_8$ $[M + H]^+$ *m/z* 482.2251 Found: $[M + H]^+$ *m/z* 482.2274. Analytical HPLC (t_R = 9.96 min, method 2).

Tert-butyl {4-[3-(4-Amino-phenyl)-2-(bis-*tert*-butoxycarbonylmethyl-amino)-propyl]-7-*tert*-butoxycarbonylmethyl-[1,4,7]triazanonan-1-yl}-acetate (4)

To a solution of **2** (26) (90 mg, 0.12 mmol) in MeOH (10 mL) was added 10% Pd/C catalyst (20 mg). The resulting mixture was subjected to hydrogenolysis by agitation with excess H_2 (g) at 20 psi in a Parr hydrogenator apparatus at ambient temperature for 14 h. The reaction mixture was filtered through Celite®, and the filtrate was concentrated *in vacuo* to provide pure **4** (81 mg, 92%). ^{1}H NMR ($CDCl_3$) δ 1.42 (s, 9 H), 1.44 (s, 18 H), 1.47 (s, 9 H), 2.02-2.60 (m, 6 H), 2.65-2.96 (m, 12 H), 3.30-3.80 (m, 8 H), 6.60 (d, 2 H), 6.91 (d, 2 H); ^{13}C NMR ($CDCl_3$) 28.1, 34.7, 51.6, 52.2, 53.0, 53.2, 56.8, 57.7, 60.2, 80.5, 80.7, 115.2, 128.9, 129.9, 144.3, 170.0, 170.6, 170.8. HRMS (Positive ion FAB) Calcd for $C_{39}H_{67}N_5O_8$ $[M + H]^+$ *m/z* 734.5068. Found: $[M + H]^+$ *m/z* 734.5029. Analytical HPLC (t_R = 27.46 min, method 1).

Tert-butyl {4-[3-(4-Amino-phenyl)-2-(*tert*-butoxycarbonylmethyl-amino)-propyl]-7-tert-butoxycarbonylmethyl-[1,4,7]triazonan-1-yl}-acetate (5)

To a solution of **3** (180 mg, 0.28 mmol) in MeOH (20mL) was added 10% Pd/C catalyst (36 mg). Compound **5** (167mg, 97%) was isolated using the same procedure described for synthesis of **4**. ^{1}H NMR ($CDCl_3$) δ 1.37 – 1.50 (m, 36 H), 2.24-2.49 (m, 5 H), 2.61-2.94 (m, 12 H), 3.28-3.47 (m, 8 H), 6.60 (d, 2 H), 6.92 (d, 2 H); ^{13}C NMR ($CDCl_3$) 28.05, 28.15, 38.23, 49.53, 55.09, 55.41, 56.74, 59.11, 62.23, 80.60, 80.75, 115.19, 128.38, 129.91, 144.76, 171.16, 171.41; HRMS (Positive ion FAB) Calcd for $C_{33}H_{58}N_5O_6$ $[M + H]^+$ *m/z* 620.4387. Found: $[M + H]^+$ *m/z* 620.4385. Analytical HPLC (t_R = 27.46 min, method 1).

{4-[3-(4-Amino-phenyl)-2-(bis-carboxymethyl-amino)-propyl]-7-carboxymethyl-[1,4,7] triazanonan-1-yl}-acetic acid (6)

Compound **4** (50 mg, 0.07 mmol) was treated with 4M HCl in 1, 4-dioxane (5 mL) at 0 °C. The resulting solution was lyophilized to provide pure **6** as a pale yellow solid (44 mg,

93%): ^{1}H NMR (D_2O) δ 2.90-3.20 (m, 6 H), 3.30-3.57 (m, 11 H), 3.72 (t, 2 H), 3.92-4.22 (m, 7 H), 4.39 (d, 1 H), 7.37 (dd, 4 H); ^{13}C NMR (D_2O) δ 33.5, 48.5, 50.2, 50.7, 51.0, 52.0, 52.7, 52.91, 53.4, 53.9, 55.9, 60.8, 123.7, 129.3, 131.0, 135.6. HRMS (Positive ion FAB) Calcd for $C_{23}H_{36}N_8O_8$ $[M + H]^+$ *m/z* 510.2587. Found: $[M + H]^+$ *m/z* 510.2564. Analytical HPLC (t_R = 5.45 min, method 2; t_R = 4.74 min, method 1).

{4-[3-(4-Amino-phenyl)-2-(carboxymethyl-amino)-propyl]-7-carboxymethyl-[1,4,7] triazonan-1-yl}-acetic acid (7)

Compound **5** (55 mg, 0.09 mmol) was treated with 4M HCl in 1, 4-dioxane (5 mL) at 0 °C. Compound **7** (48 mg, 97%) was obtained using the same procedure described for **6**. ^{1}H NMR (D_2O) δ 2.42-2.53 (m, 2 H), 2.75-3.22 (m, 14 H), 3.51 (s, 1 H), 3.75-3.95 (m, 8 H), 7.29 (dd, 4 H); ^{13}C NMR (D_2O) δ 33.7, 44.9, 48.7, 49.5, 50.9, 51.6, 55.9, 56.3, 56.7, 58.7, 123.7, 129.1, 130.8, 136.4, 169.1, 171.1, 171.8. HRMS (Positive ion FAB) Calcd for $C_{21}H_{34}N_5O_6$ $[M + H]^+$ *m/z* 452.2509. Found: $[M + H]^+$ *m/z* 452.2491. Analytical HPLC (t_R = 1.70 min, method 2).

{4-[2-(Bis-carboxymethyl-amino)-3-(4-isothiocyanato-phenyl)-propyl]-7-carboxymethyl-[1,4,7]triazanonan-1-yl}-acetic acid (8)

To a solution of **6** (20 mg, 0.031 mmol) in water (2 mL) was added a 1M solution of thiophosgene in $CHCl_3$ (0.39 mL). The resulting mixture was stirred for 2 h at room temperature. The aqueous layer was decanted, and $CHCl_3$ layer was separated and washed with water (2 × 1 mL). The combined aqueous layers were lyophilized to provide **8** as a pale yellow solid (18 mg, 85%): ^{1}H NMR (D_2O) δ 2.95-4.40 (m, 27 H), 7.18-7.42 (s, 4 H). HRMS (Positive ion FAB) Calcd for $C_{24}H_{34}N_5O_8S$ $[M + H]^+$ *m/z* 552.2117. Found: $[M + H]^+$ *m/z* 552.2128. Analytical HPLC (t_R = 14.56 min, method 2).

{4-Carboxymethyl-7-[2-(carboxymethyl-amino)-3-(4-isothiocyanato-phenyl)-propyl]-[1,4,7] triazonan-1-yl}-acetic acid (9)

To a solution of **7** (20 mg, 0.031 mmol) in water (2 mL) was added a 1M solution of thiophosgene in $CHCl_3$ (0.39 mL). Compound **9** (19 mg, 88%) was isolated using the same procedure described for **3**. ^{1}H NMR (D_2O) δ 2.52-2.60 (m, 2 H), 2.85-3.32 (m, 15 H), 3.74-3.88 (m, 8 H), 7.21 (dd, 4 H). HRMS (Positive ion FAB) Calcd for $C_{22}H_{32}N_5O_6S$ $[M + H]^+$ *m/z* 494.2073 Found: $[M + H]^+$ *m/z* 494.2081. Analytical HPLC (t_R = 16.0 min, method 1).

General procedure for the preparation of Gd(III) complexes (C-DOTA, C-NETA, or C-NE3TA)

Ligand (2 mM, 1 mL) and $GdCl_3$ (2 mM, 0.9 mL) were mixed and heated at 90 °C, while pH of the solution was constantly maintained at pH 7 by adding 1N NaOH. The heating was continued until no free Gd(III) was detected using arsenazo III (AAIII) solution. The Gd^{3+} complexes were prepared by reacting the aqueous solution of the appropriate ligand (2 mM, 1 mL, *C*-NETA, *C*-NE3TA, or *C*-DOTA) and $GdCl_3$ (2 mM, 0.9 mL) at a 1:0.9 mole ratio at 90 °C overnight, and the pH of the resulting solution was adjusted to ~7 using 1M NaOH. No unbound Gd(III) was detected in the solution as evidenced by AAIII assay and TLC analysis. The Gd complexes were purified using semi-HPLC (Method 4). Fractions centered at 20.4 min, 18.0 min, 14.5-15.1 min were collected to provided *C*-NETA, *C*-NE3TA, and *C*-DOTA, respectively. Analytical HPLC of the isolated complexes (method 5) was performed, and the data were compared to those of free ligands (Gd-*C*-NETA, t_R = 20.4 min; Gd-*C*-NE3TA, t_R = 18.0 min; Gd-*C*-DOTA, t_R = 15.4 min; *C*-NETA, t_R = 11.2 min; *C*-NE3TA, t_R = 14.2 min; *C*-DOTA, t_R = 21.6 min).

Procedure for detection of free Gd(III) using AAIII assay

AAIII assay was used for the determination of the free Gd(III) in the complex solution (27). A solution of AAIII (10μM) was prepared in the acetate buffer (NH_4OAc, 0.15 M, pH 7). Droplets of AAIII (100 μL) were arranged in a 96 well plate, and a droplet of reaction mixture (100 μL) was added to AAIII solution in each well. The presence of free Gd(III) was indicated by the immediate color change from pink to green.

ICP-MS

To verify the concentration of Gd(III) in the purified complexes, ICP-MS was performed using a computer-controlled Thermo Elemental (Now Thermo Fisher) PQ ExCell Inductively Coupled Plasma Mass Spectrometer. Samples were prepared by nitric acid digestion (9:1 nitric acid:sample) in a 65 °C water bath. The digested samples were diluted into 15 mL conical vials with a final concentration of 3% (v/v) nitric acid. Gd(III) standards were prepared in 3% (v/v) nitric acid with values 0.1, 0.25, 0.5, 1, 5, 10, 25, and 50 ng/mL Gd(III). Indium was spiked into every sample (including standards) for a final indium concentration of 5 ng/mL. Isotopes ^{157}Gd and ^{115}In were used for determination.

Relaxivity Measurements

Relaxivity measurements were acquired by taking the slope of a plot of 1/T1 (s^{-1}) versus concentration (mM). The longitudinal water proton relaxation times (T1) were determined using a Bruker mq60 NMR (Bruker Canada, Milton, ON, Canada) analyzer operating at 59.97 MHz and 37 °C. The agent was added to Millipore water and serially diluted by 0.5 to give a series of 5 concentrations (500 μL total volume) for each relaxivity trial. The T_1 relaxivity was determined using an inversion recovery pulse sequence with 10 different pulse separations per sample, 4 repetitions per echo time, phase cycling, and a recycle delay that is ≥5 times the T_1 of each given sample. All curves were fit using a mono-exponential curve fitting formula.

Radiolabeling of ligands

Each of the radionuclides (1-3 mCi in 10-20 μL of 0.1 M HCl solution) was added to 100 μL of 0.15 M NH_4OAc buffer solution (pH 4.5). 5M NH_4OAc (pH 7.3) was added as needed to adjust pH to 4.5, and the volume of the solution was brought up to 200 μL. Separate tubes containing 7 μmol of each of the ligands were prepared and the solids were dissolved in 200 μL of NH_4OAc (pH 4.5). The ligand solution was added to the radionuclide solution and the resulting tube was capped. The reactions were heated at 80 °C for 12 h, after which they were loaded onto a column of Chelex-100 resin (100-200 mesh, Na^+ form, Biorad, Richmond, CA; 1 mL volume bed, equilibrated with PBS, pH 7.4). The complexes were eluted from the resin with PBS, pH 7.4 while the resin retained the free metals.

In vitro stability of the radiolabeled metal complexes

The stability of the purified radiolabeled complexes was evaluated in human serum (Gemini Bioproducts, Woodland, CA) for up to 11 days. The serum stability of the radiolabeled complexes was assessed by measuring the transfer of the radionuclide from each complex to serum proteins using SE-HPLC methods. Radiolabeled complexes were diluted to an appropriate volume that allowed for preparation of multiple samples containing 5-10 μCi and were filter-sterilized using a Millex-GV 0.22 μm filter. This stock solution was then mixed with 1400 μL of sterile normal human serum. Aliquots (200 μL) were drawn and separated into individual tubes for subsequent analysis using aseptic technique. The samples were incubated at 37 °C, and at designated intervals, subjected to analysis by SEHPLC. Samples were loaded onto the HPLC and eluted with PBS, pH 7.4 isocratically at 1 mL/min. Radioactivity still associated with the chelate typically displayed a retention time of ~8.5 min

at this flow rate. Radioactivity associated with a transfer to serum proteins generally appeared at ~6 min.

In vivo biodistribution studies of the radiolabeled metal complexes

Female athymic mice were obtained from Charles River Laboratories (Wilmington, MA) at 4-6 weeks of age. The pH of the radiolabeled ligands was adjusted to pH ~7.0 with 0.5 M sodium bicarbonate (pH 10.5) and diluted in phosphate-buffered saline. The radiolabeled ligands (5-10 μCi for ^{86}Y, $^{205/6}$Bi, ^{177}Lu, and ^{203}Pb) were administered to the mice in 200 μL of solution *via* tail vein injection. The mice (5 per data point) were sacrificed by exsanguination at 0.5, 1, 4, 8, and 24 h. Blood and the major organs were harvested, wet-weighed and the radioactivity measured in a γ-scintillation counter (1480 Wizard, Perkin Elmer). The percent injected dose per gram (% ID/g) was determined for each tissue. The values presented are the mean and standard deviation for each tissue. All animal experiments were performed in compliance with current regulations and guidelines of the U.S. Dept. of Agriculture and approved by the NCI Animal Care and Use Committee.

General Procedure for Spectroscopic Determination of Ligand to Protein Ratio

A stock solution of the Cu(II)-AAIII reagent was prepared in 0.15 M NH_4OAc, pH 7.0 by adding an aliquot of a 5.00×10^{-4} M Cu(II) atomic absorption solution (to afford a 5 μM solution of copper) to a 10 μM solution of arsenazo III. This solution was stored in the dark to avoid degradation over time. A UV/Vis spectrometer was zeroed against a cuvette filled with 1.0 mL of a 0.15 M NH_4OAc solution at pH 7.0 with a window open from 250 nm to 700 nm. The acetate solution was removed and replaced with 1.0 mL of the Cu(II)-AAIII reagent, a spectrum was collected and the absorbance values at 280 and 652 nm noted. 50 μL of the Cu (II)-AAIII reagent were removed and discarded. The ligand-antibody conjugate of interest was added (50 μL) and the spectrum was immediately collected. Spectra were then collected periodically until no further change was noted for the peaks at 280 and 652 nm (less than 30 min for the Cu(II)-AAIII reagent with the ligands detailed in this paper). A series of calculations detailed in the discussion allow for the determination of the concentration of ligand in the sample.

Spectroscopic Determination of Ligand to Protein Ratio

All absorbance measurements were obtained on an Agilent 8453 diode array spectrophotometer equipped with a 8-cell transport system (designed for 1 cm cells). Metal-free stock solutions of all buffers were prepared using Chelex-100 resin (100-200 mesh, Bio-Rad Lab, Hercules, CA). Chelex resin (5 g) was added into the buffer solution (500 mL) and the mixture was shaken for 1 h in a shaker, stored in the refrigerator overnight, and filtered through a Corning filter system (#430513, pore size 0.2 μM). Disposable PD-10 Sephadex™ G-25M columns (GE Healthcare, Piscataway, NJ) were rinsed with 25 mL of the appropriate buffer prior to addition of antibody or its ligand conjugates. Centricon C-50 (50,000 MWCO) Centrifugal Filter Devices were purchased from Amicon Bioseparations (Millipore, Bedford, MA) and were rinsed several times with DI H_2O prior to use. Trastuzumab was purchased from Genentech Inc. (South San Fransico, CA). The initial concentration of Trastuzumab was determined by the Lowry method (24). Phosphate buffered saline (PBS) was purchased from Gibco as a 1× solution at pH 7.4 and was used as received. Ammonium acetate (0.15 M, pH 7.0 and 0.15 M, pH 4.5), bicarbonate buffer (50 mM $NaHCO_3$, 150 mM NaCl, 10 mM EDTA, pH 8.5), and conjugation buffer (50 mM HEPES, 150 mM NaCl, pH 8.6) were prepared as 10× solutions, chelexed and then diluted to 1X solutions for use as needed with DI H_2O. Phosphate buffered saline (PBS), 1X, pH 7.4 consisted of 0.08 M Na_2HPO_4, 0.02 M KH_2PO_4, 0.01 M KCl, and 0.14 M NaCl.

Conjugation of C-NETA-NCS to Trastuzumab

Trastuzumab (9.5 mg) was added to a PD-10 column previously charged with bicarbonate buffer. Additional buffer was added in 0.5 mL portions to the PD-10 column to exchange the buffer solution of the antibody. The buffer solution collected between 3.5 and 5.0 mL was combined following confirmation of the presence of Trastuzumab via analysis of the UV/VIS spectrum at 280 nm. To a sterile test tube containing the recovered Trastuzumab (5 mg) was added a 20-fold excess of *C*-NETA-NCS. The resulting solution was gently agitated overnight at room temperature. The following day, this solution was placed on a Centricon C-50 membrane and spun down to reduce volume. PBS (3 × ~2 mL) was added to the remaining solution of the C-NETA-Trastuzumab conjugate, followed by centrifugation in order to remove unreacted ligand. The volume of purified, conjugate antibody was brought to 2.00 mL with PBS. The ligand to protein (L/P) ratio was determined by measuring the absorbance of the solution at 280 nm, which indicated that 1.45 mg (9.67×10^{-6} M, 29%) of the Trastuzumab remained after centrifugation. An aliquot of the C-NETA-Trastuzumab conjugate (50 μL) was added to the cuvette containing the Cu(II)-AAIII reagent (950 μL) and the absorbance at 652 nm was monitored over time. The reaction was complete after 20 min, and the concentration of *C*-NETA-NCS was calculated (1.48×10^{-5} M). The L/P for the C-NETA-Trastuzumab conjugate was found to be 1.5 to 1.

Conjugation of C-NE3TA-NCS to Trastuzumab

Trastuzumab (6.0 mg, 2.5 mL) was added to a PD-10 column previously charged with conjugation buffer. Additional conjugation buffer (3.5 mL) was added to PD-10 column to exchange the buffer solution of the antibody. The collected antibody solution (5.9 mg, 98.0%) was then added to a 10-fold excess of *C*-NE3TA-NCS. The solution was gently agitated for 24 h at room temperature. The reaction solution was then placed on a Centricon C-50 membrane and spun down to reduce volume. PBS (3×2 mL) was added to the remaining solution of the *C*-NE3TA-Trastuzumab conjugate, followed by centrifugation to remove unreacted ligand. The volume of purified conjugate antibody was brought to 1 mL with PBS. The analysis of the absorbance of the solution at 280 nm indicated that 5.71 mg (38.8×10^{-5} M, 96.8%) of the Trastuzumab remained after the processing.

A stock solution of the Cu(II)-AAIII reagent was prepared in 0.15 M NH_4OAc, pH 7.0 by adding an aliquot of a 5 μM Cu(II) atomic absorption solution to a 10 μM solution of AAIII. This solution was stored in the dark to avoid degradation over time. A UV/Vis spectrometer was zeroed against a cuvette filled with 2.0 mL of a 5 μM AAIII solution at pH 4.5 with a window open from 200 nm to 1100 nm. The AAIII solution was removed and replaced with 2.000 mL of the Cu(II)-AAIII reagent, a spectrum was collected and the absorbance values at 610 nm noted. Solutions of *C*-NE3TA-NO_2 were then used for generating the calibration graph. Various concentration of *C*-NE3TA-NO_2 solution (50 μL) was reacted with 1.95 mL of the Cu (II)-AAIII reagent at room temperature. Abosrbance measurements at 610 nm were taken after 5 min. An aliquot of the *C*-NE3TA-Trastuzumab conjugate (50 μL) was added to a cuvette containing the Cu(II)-AAIII reagent (1.95 mL) and the absorbance at 610 nm was monitored over time. Spectra were then collected periodically until no further change was noted for the peaks at 280 and 610 nm. The reaction was complete after 30 min, and the concentration of *C*-NE3TA was calculated (9.7×10^{-5} M). The L/P for the *C*-NE3TA-Trastuzumab conjugate was found to be 2.5 to 1.

Results and discussion

Synthesis of C-NETA and C-NE3TA

C-NE3TA was serendipitously discovered during the synthesis of *C*-NETA. C-NE3TA contains four amines and three carboxylates as potential donor groups. The heptadentate C-

NE3TA forms a neutral complex with Y(III), Lu(III), Bi(III), and Gd(III) that requires no counter-ion and thus these formed complexes have an advantage of less protein interaction and a potentially more favorable *in vivo* tissue distribution. Synthesis of *C*-NE3TA is shown in Scheme 1. As an initial attempt to prepare *tert*-Butyl *C*-NETA **2** (26), the free amino groups in **1** (26) were reacted with *tert*-butyl bromoacetate in CH_3CN in the presence of diisopropylethylamine (DIPEA) as a base. However, the reaction afforded **2** in low (<35%) and non-reproducible yields. The reaction also provided a significant amount of polyalkylated by-products very difficult to differentiate from **2** by TLC as confirmed by NMR. To improve the synthesis of **2**, starting material **1** as a HCl salt instead of free amine was directly reacted with *tert*-butyl bromoacetate in DMF at 50 °C (Scheme 1) (20). Surprisingly, the reaction provided *tert*-butyl C-NE3TA **(3)** in 68% yield as the major product along with a small amount of **2**. This result was taken as an indication that the formation of **2** requires an elevated reaction temperature. Indeed, when starting material **1**, still as a HCl salt, was reacted with *tert*-butyl bromoacetate in DMF at 90 °C (26), **2** was obtained in an improved yield (54%). Although not described in detail in this paper, the preparation of **2** and **3** was not straightforward. Numerous reaction conditions varying solvents, bases, temperatures, mole ratios of the reagents were investigated. Purification of **2** and **3** using flash silica gel (or alumina) column chromatography was found to be quite challenging due to the presence of by-products, specifically polyalkylated by-products which could not be resolved from the desired ligands by TLC. Significant amount of solvents were consumed even in small-scale column chromatographic purifications of **2** (~100 mg) using a very gradual increase of solvent polarity. With the challenge encountered in isolation of **2** and **3** in high purity, development of a reliable and efficient purification method available for preparation of these intermediates, **2** and **3**, in high purity so that after deprotection of the tert-butyl groups, the water soluble per-acid products could be cleanly isolated. Semi-preparative HPLC of the reaction mixture containing **2** and **3** eluted with a binary gradient (solvent A = 0.05 M AcOH/Et_3N, pH 6.0 and solvent B = CH_3CN) successfully separated **2** and **3** in high purity. The desired ligands, *C*-NETA (26) and *C*-NE3TA were then obtained by removal of the *tert*-butyl groups of **2** and **3** using HCl(g) in 1,4-Dioxane. Synthesis of *C*-NE3TA-NCS and *C*-NETA-NCS having a functional linker for conjugation to an antibody is shown in Scheme 2. The nitro group in **2** and **3** was transformed into the amino group to provide **4** and **5**, respectively. Removal of the *tert*-butyl groups in **4** and **5** followed by reaction with thiophosgene provided the desired ligands with the linker for conjugation to antibody, *C*-NETA-NCS (**8**) and *C*-NE3TA-NCS (**9**).

Relaxivities

The Gd(III) complexes of the new chelates in the nitro form were prepared and purified. The T1 relaxivity of Gd(*C*-NETA) and Gd(*C*-NE3TA) was measured and compared to that of Gd(*C*-DOTA). Previously, we reported the Gd(III) complex of non-functionalized bimodal ligand NETA to be stable in both serum and in vivo and displayed considerably enhanced T1 relaxivity compared to Gd(DOTA) where the Gd(III) is coordinated to the eight donor atoms of the ligands with one vacant coordination site available to bind a water molecule (q =1) (2). The increase in relaxivity of Gd(NETA) as compared to Gd(DOTA) was proposed to be ascribed to a decrease in ligand denticity from eight to seven-coordinate by one of the flexible acyclic pendant coordinating groups not being coordinated at all or from an “on”-“off” mechanism of one of the pendant coordinating groups and thus resulting in an increase in q value of the Gd(NETA) complex to an intermediate state between one coordinated water molecule (q=1) and two coordinated water molecules (q=2) (18). In the present study, the Gd(III) complexes of bifunctional ligands *C*-NETA and heptadentate *C*-NE3TA were prepared as potential MRI contrast agents. Heptadentate *C*-NE3TA was expected to provide enhanced relaxivity due to increase in hydration number (*q*) when compared to *C*-NETA and *C*-DOTA. The Gd(III) complexes of the bifunctional ligands were prepared and purified using semi-preparative HPLC, while the presence of free Gd(III) ions was detected using an ArsenazoIII (AAIII) assay

(27). Relaxivity of the aqueous Gd(III) complexes (~pH 7) were measured on a Bruker MQ60 NMR analyzer, and the concentration of the Gd(III) complexes was measured by ICP-MS. The relaxivity data (Figure 2) indicate that Gd-*C*-NETA (4.77 $mM^{-1}s^{-1}$) and Gd-*C*-NE3TA (5.89 $mM^{-1}s^{-1}$) complexes provided higher relaxivity as compared to the DOTA complex (3.96 $mM^{-1}s^{-1}$). Introduction of a functional nitro group into the NETA backbone did not impact the T1 relaxivity of NETA. The difference of T1 relaxivity (~1 MHz) between *C*-DOTA and *C*-NETA was similar to that between DOTA and NETA. As mentioned above, the on and off binding to Gd(III) of one of the pendant coordinates would have resulted in enhanced relaxivity of Gd(*C*-NETA) as compared to Gd(*C*-DOTA). Among the evaluated Gd(III) complexes, Gd (*C*-NE3TA) gives the highest T1 relaxivity at 60 MHz, probably due to an increase in q (21). The relaxation rates for the Gd(III) chelates are dominated by the inner-sphere dipolar coupling between the coordinated water molecule and the paramagnetic Gd(III). The measured relaxivities arise from the exchange between the coordinated water molecule and the surrounding water molecules in solution (21). An increase in the number of coordinated water molecules to the Gd(III), which could have occurred with dissociation of Gd(III) from the chelate in solution, would have resulted in a significant increase in the measured relaxivities. No indication of Gd(III) dissociation is evident from the relaxivity data, which is in agreement with the *in vitro* serum stability and *in vivo* biodistribution studies.

In vitro serum stability

C-NETA and *C*-NE3TA were radiolabeled with ^{90}Y, ^{177}Lu, ^{203}Pb, $^{205/6}Bi$, or ^{153}Gd as previously described (17,18). *In vitro* serum stability of the radiolabeled complexes purified via ion-exchange chromatography was performed to determine if *C*-NETA or *C*-NE3TA labeled with the radionuclides remained stable without transchelation or loss of their respective radionuclide in human serum. This was assessed by measuring the transfer of radionuclide from the complex to serum proteins over the course of 11 days. *C*-NETA and *C*-NE3TA radiolabeled with ^{90}Y, ^{177}Lu, $^{205/6}Bi$, and ^{153}Gd were stable in serum for up to 11 days with no measurable loss of radioactivity. However, considerable release of radioactivity into serum (~17%) over 7 days was observed with the ^{203}Pb-labeled *C*-NETA. ^{203}Pb-*C*-NE3TA was also unstable by this assay as indicated by significant amounts of ^{203}Pb (~40%) dissociating within 1 day.

In vivo biodistribution

The *in vivo* stability of the radiolabeled complexes was evaluated by performing biodistribution studies in normal athymic mice. The results of the biodistribution studies for the radiolabeled complexes are shown in Tables 2-5. Selected organs and the blood were harvested at 5 time points, 0.5, 1, 4, 8, and 24 h post-injection. *C*-NETA (26) and *C*-NE3TA radiolabeled with ^{177}Lu have similar biodistribution profiles, and both complexes were rapidly cleared from the blood and displayed low radioactivity levels in all organs (<0.8% ID/g at 24 h, Table 2). ^{86}Y-*C*-NETA and ^{86}Y-*C*-NE3TA resulted in rapid blood and liver clearance (Table 3). ^{86}Y-*C*-NETA displayed relatively higher uptake at the femur as compared to that of ^{86}Y-*C*-NE3TA at all time points (0.78±0.07% ID/g *Vs* 0.08±0.02% ID/g at 24 h, respectively). Low radioactivity levels in other organs were observed with both complexes. *C*-NE3TA radiolabeled with $^{205/6}Bi$ was rapidly cleared from the blood, lung, heart, and femur and displayed a higher radioactivity level in the kidney when compared to the other organs (Table 4). The radioactivity level of $^{205/6}Bi$-*C*-NE3TA in the kidney peaked at 5.05 ± 0.24 %ID/gm at 0.5 h and decreased to 0.73 ± 0.19 %ID/gm by 24 h. $^{205/6}Bi$-*C*-NETA exhibited extremely rapid blood clearance and low radioactivity levels at all of the organs except the kidney (< 1.0% ID/g at all time points) while radioactivity in the kidney decreased rather slowly starting from 24.9% ± 3.48 ID/g to 6.06 ± 0.19 at 24 h (26). *C*-NE3TA radiolabeled with ^{153}Gd almost completely cleared from the blood, liver, spleen, lung, heart, and femur in less than 4 h, with the radioactivity level in the kidney was 0.16% ± 0.11 ID/g at 24 h post-injection (Table

5). ^{153}Gd-*C*-NETA also displayed extremely rapid blood clearance and low uptake at spleen and lung, and heart, while relatively increased radioactivity levels in the liver, kidney, and femur at 24 h (2.98 ± 0.44 % ID/g, 2.18 ± 0.14 % ID/g, 2.31 ± 0.40 % ID/g, respectively) were observed with this complex (Table 5).

Conjugation of *C*-NETA-NCS and *C*-NE3TA-NCS to Trastuzumab and Determination of L/P ratio based on Cu(II)-AA(III) assay

HER2 are receptors over-expressed in a variety of epithelial tumors making this an attractive target. Trastuzumab, a monoclonal antibody thatselectively targets the HER2 protein and blocks its over-expression function (22) and has been shown to enhance a survival rate of metastatic breast cancer patients was chosen as a tumor targeting biomolecule (23) for the present study. *C*-NETA was conjugated with Trastuzumab by an established method (24). Protein concentration was quantified by the method of Lowry (25). The Cu(II)-AAIII based UV-Vis spectrophotometric assay as described previously (24) was used for the determination of the number of *C*-NETA ligands linked to Trastuzumab (L/P ratio). The L/P ratio for *C*-NETA-Trastuzumab and *C*-NE3TA conjugates was found to be 1.5 and 2.5, respectively.

Conclusions

The novel bifunctional ligands, octadentate *C*-NETA and heptadentate *C*-NE3TA were synthesized for use in RIT and MRI applications. The T1 relaxivities of their corresponding Gd(III) complexes are reported. At clinically relevant field strength, the relaxivities of Gd(*C*-NETA) and Gd(*C*-NE3TA) are higher than that of a bifunctional version of the clinically used contrast agent, Gd(DOTA). The *in vitro* serum stability and *in vivo* biodistribution data of the ^{153}Gd-labeled complexes, Gd(*C*-NETA) and Gd(*C*-NE3TA), indicate that *C*-NETA and *C*-NE3TA bind ^{153}Gd with high complex stability. *C*-NETA and *C*-NE3TA were evaluated as chelators of ^{177}Lu, ^{90}Y, ^{212}Pb, ^{212}Bi, or ^{213}Bi for RIT applications. *C*-NETA and *C*-NE3TA radiolabeled with ^{177}Lu, ^{90}Y, and $^{205/6}$Bi were extremely stable without loss of any radioactivity from the metal complex in human serum for up to 11 days. Both ^{203}Pb-*C*-NETA and ^{203}Pb-*C*-NE3TA underwent significant dissociation of the metal from the complexes. *In vivo* biodistribution of *C*-NETA and *C*-NE3TA labeled with ^{177}Lu or ^{90}Y using athymic mice indicate that the radiolabeled complexes exhibited rapid blood clearance and relatively low radioactivity levels in the normal organs and possess a favorable biodistribution profile. $^{205/6}$Bi-*C*-NE3TA exhibited extremely rapid blood clearance and low radioactivity level in the normal organs at 24 h. $^{205/6}$Bi-*C*-NETA displayed a minimum amount of uptake of the activity in the normal organs except for the kidney. High renal uptake of the activity at all time points was observed with $^{205/6}$Bi-*C*-NETA. The bifunctional ligands, *C*-NETA and *C*-NE3TA were successfully conjugated to trastuzumab with the respective L/P product ratio of 1.5 and 2.5 as determined using a UV/Vis spectrophotometric AAIII assay. The result of T1 relaxivity, *in vitro* serum stability, and *in vivo* biodistribution studies suggests that the novel bifunctional ligands, *C*-NETA and *C*-NE3TA are promising bifunctional ligands for disease-specific Gd(III)-based MRI and RIT of ^{177}Lu and ^{90}Y.

Acknowledgements

We acknowledge financial support from the National Institutes of Health (K22CA102637 and R01CA112503-01A2 to CHS). This research was supported in part by the Intramural Research Program of the NIH, National Cancer Institute, Center for Cancer Research. We thank Dr. Thomas Meade for the NMR analyzer and Mr. Keith Macrenaris for the ICP-MS data.

References

1. Knox SJ, Meredith RF. Clinical radioimmunotherapy. Sem. Radiat. Oncol 2000;10:73–93.

2. Caravan P, Ellison JJ, McMurry TJ, Lauffer RB. Gadolinium(III) Chelates as MRI Contrast Agents: Structure, Dynamics, and Applications. Chem. Rev 1999;99:2293–2352. [PubMed: 11749483]
3. Yoneda S, Emi N, Fujita Y, Ohmichi M, Hirano S, Suzuki KT. Effects of gadolinium chloride on the rat lung following intratracheal instillation. Fundam. Appl. Toxicol 1995;28:65–70. [PubMed: 8566485]
4. McDevitt MR, Ma D, Lai LT, Simon J, Borchardt P, Frank RK, Wu K, Pellegrini V, Curcio MJ, Miederer M, Bander NH, Scheinberg DA. Tumor therapy with targeted atomic nanogenerators. Science 2001;294:1537–40. [PubMed: 11711678]
5. Srivastava S, Dadachova E. Recent advances in radionuclide therapy. Semin Nucl Med 2001;31:330–41. [PubMed: 11710775]
6. Milenic DE, Brady ED, Brechbiel MW. Antibody-targeted radiation cancer therapy. Nat. Rev. Drug Discov 2004;3:488–99. [PubMed: 15173838]
7. Borghaei H, Schilder RJ. Safety and efficacy of radioimmunotherapy with yttrium 90 ibritumomab tiuxetan (Zevalin). Semin. Nucl. Med 2004;34(S1):4–9. [PubMed: 14762738]
8. Jhanwar YS, Divgi CJ. Current status of therapy of solid tumors. Nucl. Med 2005;46(S1):141S–50S.
9. Hassfjell S, Brechbiel MW. The development of the α-particle emitting radionuclides ^{212}Bi and ^{213}Bi, and their decay chain related radionuclides for therapeutic applications. Chem. Rev 2001;101:2019–36. [PubMed: 11710239]
10. Lewis MR, Raubitschek A, Shively JE. A facile, water-soluble method for modification of proteins with DOTA. Use of elevated temperature and optimized pH to achieve high specific activity and high chelate stability in radiolabeled immunoconjugates. Bioconjugate Chem 1994;5:565–76.
11. Chakrabarti MC, Le N, Paik CH, De Graff WG, Carrasquillo JA. Prevention of radiolysis of monoclonal antibody during labeling. J. Nucl. Med 1996;37:1384–8. [PubMed: 8708780]
12. Liu S, Edwards DS. Bifunctional chelators for therapeutic lanthanide radiopharmaceuticals. Bioconjugate Chem 2001;12:7–34.
13. Raymond KN, Pierre VC. Next generation, high relaxivity gadolinum MRI agents. Biconjugate Chem 2005;16:3–8.
14. Banci, L.; Bertini, I.; Luchinat, C. Nuclear and Electronic Relaxation. VCH; Weinheim: 1991.
15. Yoneda S, Emi N, Fujita Y, Ohmichi M, Hirano S, Suzuki KT. Effects of gadolinium chloride on the rat lung following intratracheal instillation. Fundam. Appl. Toxicol 1995;28:65–70. [PubMed: 8566485]
16. Chong HS, Garmestani K, Milenic D, Brechbiel MW. Design, Synthesis, and Biological Evaluation of Novel Macrocycles with Pendant Donor Groups as Radioimmunotherapy (RIT) agents. J. Med. Chem 2002;45:3458–64. [PubMed: 12139456]
17. Chong HS, Milenic DE, Garmestani K, Brady ED, Arora H, Pfiester C, Brechbiel MW. In vitro and in vivo evaluation of novel ligands for radioimmunotherapy. Nucl. Med. Biol 2006;33:459–67. [PubMed: 16720237]
18. Chong HS, Garmestani K, Bryant LH Jr. Milenic DE, Overstreet T, Birch N, Le T, Brady ED, Brechbiel MW. Synthesis and Evaluation of Novel Macrocyclic and Acyclic Ligands as Contrast Enhancement Agents for Magnetic Resonance Imaging. J. Med. Chem 2006;49:2055–62. [PubMed: 16539394]
19. Chong HS, Song HA, Birch N, Le T, Lim S, Ma X. Efficient synthesis and evaluation of bimodal ligand NETA. Bioorg. Med. Chem. Lett. 2008In Press
20. Ameido JC Jr, Bernard PJ, Fountain M, Wagenen GV Jr. A Practical Manufacturing Synthesis of 1-(R)-Hydroxymethyl-Dtpa: An Important Intermediate in the Synthesis of MRI Contrast Agents. Syn. Commun 1999;29:2377–91.
21. Kim WD, Kiefer GE, Maton F, McMillan K, Muller RN, Sherry AD. Relaxometry, luminescence measurements, electrophoresis, and animal biodistribution of lanthanide(III) complexes of some polyaza macrocyclic acetates containing pyridine. Inorg. Chem 1995;34:2233–43.
22. Agus DB, Bunn PA Jr. Franklin W, Garcia M, Ozols RF. HER-2/neu as a therapeutic target in non-small cell lung cancer, prostate cancer, and ovarian cancer. Semin. Oncol 2000;27:53–63. [PubMed: 11236029]

23. Pietras RJ, Pegram MD, Finn RS, Maneval DA, Slamon DJ. Remission of human breast cancer xenografts on therapy with humanized monoclonal antibody to HER-2 receptor and DNA-reactive drugs. Oncogene 1998;17:2235–49. [PubMed: 9811454]

24. Brady ED, Chong HS, Milenic DE, Brechbiel MW. Development of a spectroscopy assay for bifunctional ligand-protein conjugates based on copper. Nucl. Med. Biol 2004;31:795–802. [PubMed: 15246371]

25. Lowry OH, Rosebrough NJ, Rarr AL, Randall AJ. Protein measurement with the folin phenol reagent. J. Biol. Chem 1951;193:265–75. [PubMed: 14907713]

26. Chong HS, Ma X, Le T, Kwamena B, Milenic DE, Brady ED, Song HA, Brechbiel MW. Rational Design and Generation of a Bimodal Bifunctional Ligand for Antibody-Targeted Radiation Cancer Therapy. J. Med. Chem 2008;51:118–25. [PubMed: 18062661]

27. Barge A, Cravotto G, Gianolio E, Fedeli F. How to determine free Gd and free ligand in solution of Gd chelates. Contrast Med. Mol. Imaging 2006;1:184–8.

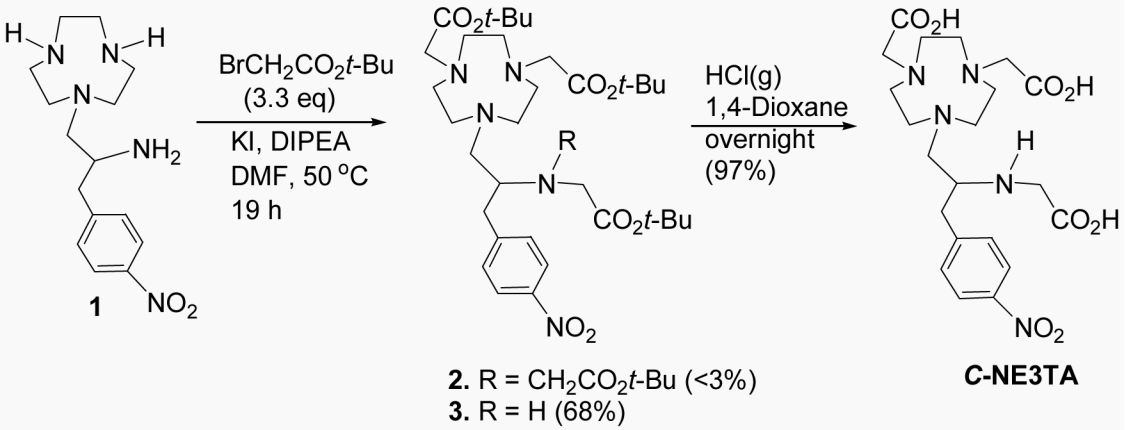

Scheme 1.
Synthesis of *C*-NE3TA

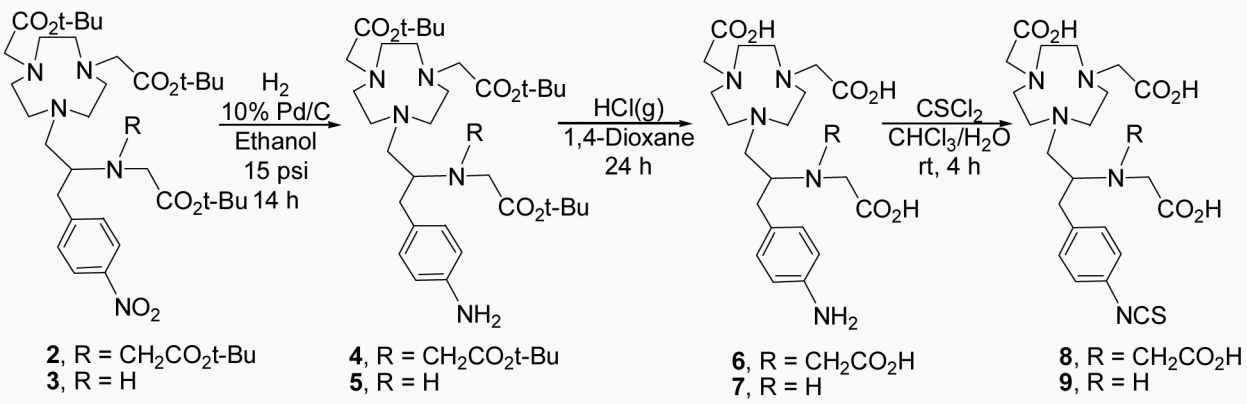

Scheme 2.
Synthesis of *C*-NETA-NCS (8) and *C*-NE3TA-NCS (9)

Table 1

In vitro serum stability of *C*-NETA and *C*-NE3TA radiolabeled with radioisotopes

Time	*C*-NE3TA					*C*-NETA				
(h)	^{177}Lu	^{90}Y	$^{205/6}$Bi	^{203}Pb	^{153}Gd	^{177}Lu*	^{90}Y	$^{205/6}$Bi*	^{203}Pb	^{153}Gd
0	100	100	100	95.1	100	100	100	100	100	100
1	100	100	100	67.5	100	100	100	100	98.1	100
2	100	100	100	59.9	100	100	100	100	98.7	100
4	100	100	100	56.1	100	100	100	100	-	100
6	100	100	100	56.1	100	100	100	100	98.0	100
22	100	100	100	-	100	100	100	100	97.0	100
26	100	100	100	65.7	100	100	100	100	-	100
92	100	100	100	75.0	100	100	100	100	-	100
96	100	100	100	-	100	100	100	100	95.7	100
118	100	100	100	77.9	100	100	100	100	95.7	100
141	100	100	100	73.2	100	100	100	100	-	100
142	100	100	100	-	100	100	100	100	91.4	100
164	100	100	100	78.2	100	100	100	100	-	100
166	100	100	100	-	100	100	100	100	82.7	100
192	100	100	100	83.7	100	100	100	100	-	100
262	100	100	100	90.9	100	100	100	100	-	100

*The data were cited for comparison (26).

Table 2

Biodistribution of ligands radiolabeled with ^{177}Lu in Non-Tumor Bearing Athymic Mice.

Ligand	Tissue	Timpoints (hr)				
		0.50	**1.00**	**4.00**	**8.00**	**24.00**
***C*-NE3TA**	Blood	0.93 ± 0.30	0.31 ± 0.04	0.12 ± 0.02	0.06 ± 0.01	0.01 ± 0.00
	Liver	0.82 ± 0.27	0.69 ± 0.20	0.50 ± 0.02	0.36 ± 0.05	0.31 ± 0.04
	Spleen	0.33 ± 0.08	0.28 ± 0.20	0.19 ± 0.07	0.13 ± 0.02	0.12 ± 0.05
	Kidney	2.78 ± 0.99	1.57 ± 0.52	1.34 ± 0.09	1.16 ± 0.19	0.84 ± 0.08
	Lung	0.87 ± 0.22	0.42 ± 0.16	0.17 ± 0.03	0.15 ± 0.03	0.07 ± 0.03
	Heart	0.37 ± 0.08	0.19 ± 0.09	0.08 ± 0.02	0.10 ± 0.11	0.02 ± 0.01
	Femur	1.06 ± 1.35	0.39 ± 0.13	0.36 ± 0.11	0.28 ± 0.15	0.38 ± 0.10
***C*-NETA** *	Blood	0.91 ± 0.41	0.34 ± 0.55	0.03 ± 0.00	0.01 ± 0.00	0.00 ± 0.00
	Liver	0.56 ± 0.21	0.25 ± 0.034	0.16 ± 0.04	0.13 ± 0.03	0.08 ± 0.01
	Spleen	0.54 ± 0.38	0.15 ± 0.11	0.07 ± 0.01	0.07 ± 0.03	0.05 ± 0.03
	Kidney	2.98 ± 1.24	1.19 ± 0.47	1.07 ± 0.20	0.87 ± 0.24	0.59 ± 0.12
	Lung	0.88 ± 0.41	0.26 ± 0.08	0.10 ± 0.06	0.04 ± 0.01	0.03 ± 0.01
	Heart	0.43 ± 0.16	0.11 ± 0.04	0.04 ± 0.01	0.03 ± 0.01	0.02 ± 0.01
	Femur	0.66 ± 0.13	0.53 ± 0.24	0.19 ± 0.05	0.17 ± 0.01	0.19 ± 0.08

Values are the percent injected dose per gram(% ID/g) ± standard deviation

* The data were cited for comparison (26).

Table 3

Biodistribution of ligands radiolabeled with ^{86}Y in Non-Tumor Bearing Athymic Mice

Ligand	Tissue	Timpoints (hr)				
		0.50	**1.00**	**4.00**	**8.00**	**24.00**
***C*-NE3TA**	Blood	1.86 ± 1.92	0.76 ± 1.09	0.05 ± 0.05	0.02 ± 0.00	0.00 ± 0.00
	Liver	1.65 ± 0.59	0.88 ± 0.59	0.17 ± 0.05	0.20 ± 0.16	0.10 ± 0.03
	Spleen	0.70 ± 0.15	0.47 ± 0.26	0.13 ± 0.08	0.07 ± 0.02	0.07 ± 0.02
	Kidney	2.58 ± 1.04	2.00 ± 2.32	0.74 ± 0.15	0.49 ± 0.10	0.35 ± 0.05
	Lung	1.64 ± 0.99	1.16 ± 0.65	0.10 ± 0.04	0.16 ± 0.22	0.23 ± 0.36
	Heart	0.79 ± 0.52	0.38 ± 0.31	0.06 ± 0.02	0.05 ± 0.01	0.02 ± 0.01
	Femur	1.19 ± 0.48	0.82 ± 0.26	0.30 ± 0.04	0.22 ± 0.06	0.08 ± 0.02
***C*-NETA**	Blood	0.63 ± 0.18	0.22 ± 0.04	0.05 ± 0.00	0.03 ± 0.00	0.03 ± 0.01
	Liver	0.48 ± 0.08	0.32 ± 0.07	0.29 ± 0.03	0.22 ± 0.03	0.17 ± 0.02
	Spleen	0.83 ± 0.50	1.02 ± 1.07	0.24 ± 0.05	0.17 ± 0.03	0.26 ± 0.03
	Kidney	2.64 ± 1.18	0.79 ± 0.43	1.12 ± 0.09	0.87 ± 0.11	0.64 ± 0.08
	Lung	0.73 ± 0.17	0.40 ± 0.06	0.17 ± 0.05	0.13 ± 0.01	0.16 ± 0.03
	Heart	0.66 ± 0.12	0.28 ± 0.06	0.22 ± 0.05	0.15 ± 0.01	0.24 ± 0.05
	Femur	1.69 ± 0.83	2.05 ± 0.20	1.79 ± 0.19	0.66 ± 0.02	0.78 ± 0.07

Values are the percent injected dose per gram(% ID/g) ± standard deviation

Table 4

Biodistribution of ligands radiolabeled with $^{205/6}$Bi in Non-Tumor Bearing Athymic Mice

Ligand	Tissue	Timpoints (hr)				
		0.50	**1.00**	**4.00**	**8.00**	**24.00**
***C*-NE3TA**	Blood	0.46 ± 0.18	0.13 ± 0.02	0.03 ± 0.00	0.02 ± 0.01	0.01 ± 0.00
	Liver	1.01 ± 0.15	0.80 ± 0.16	0.52 ± 0.13	0.37 ± 0.08	0.14 ± 0.03
	Spleen	0.45 ± 0.24	0.25 ± 0.02	0.18 ± 0.01	0.12 ± 0.02	0.13 ± 0.01
	Kidney	5.05 ± 0.24	4.69 ± 0.55	3.42 ± 0.55	1.99 ± 0.32	0.73 ± 0.19
	Lung	0.56 ± 0.13	0.25 ± 0.03	0.16 ± 0.01	0.13 ± 0.04	0.09 ± 0.01
	Heart	0.36 ± 0.09	0.19 ± 0.02	0.12 ± 0.01	0.09 ± 0.01	0.08 ± 0.02
	Femur	0.62 ± 0.27	0.26 ± 0.05	0.23 ± 0.06	0.14 ± 0.02	0.13 ± 0.01
***C*-NETA** *	Blood	0.52 ± 0.11	0.23 ± 0.07	0.09 ± 0.01	0.08 ± 0.01	0.06 ± 0.01
	Liver	1.01 ± 0.05	0.92 ± 0.11	0.68 ± 0.14	0.62 ± 0.12	0.49 ± 0.04
	Spleen	0.77 ± 0.18	0.60 ± 0.12	0.36 ± 0.12	0.41 ± 0.03	0.42 ± 0.02
	Kidney	24.91 ± 3.48	24.63 ± 2.79	17.29 ± 3.24	10.55 ± 1.38	6.06 ± 1.34
	Lung	0.85 ± 0.16	0.53 ± 0.15	0.41 ± 0.07	0.41 ± 0.06	0.33 ± 0.07
	Heart	0.55 ± 0.02	0.37 ± 0.09	0.23 ± 0.04	0.29 ± 0.04	0.20 ± 0.02
	Femur	1.25 ± 0.11	0.86 ± 0.11	0.66 ± 0.07	0.87 ± 0.07	0.47 ± 0.08

Values are the percent injected dose per gram(% ID/g) ± standard deviation

* The data were cited for comparison (26).

Table 5

Biodistribution of ligands radiolabeled with ^{153}Gd in Non-Tumor Bearing Athymic Mice

Ligand	Tissue	Timpoints (hr)				
		0.50	**1.00**	**4.00**	**8.00**	**24.00**
***C*-NE3TA**	Blood	1.41 ± 0.57	0.20 ± 0.08	0.00 ± 0.00	0.00 ± 0.00	0.00 ± 0.00
	Liver	1.74 ± 0.69	0.58 ± 0.22	0.03 ± 0.01	0.02 ± 0.00	0.02 ± 0.01
	Spleen	0.50 ± 0.37	0.24 ± 0.05	0.02 ± 0.00	0.02 ± 0.00	0.01 ± 0.01
	Kidney	4.28 ± 1.33	1.13 ± 0.12	0.52 ± 0.04	0.38 ± 0.06	0.16 ± 0.11
	Lung	0.91 ± 0.28	0.32 ± 0.09	0.03 ± 0.00	0.02 ± 0.00	0.01 ± 0.01
	Heart	0.43 ± 0.16	0.14 ± 0.06	0.01 ± 0.00	0.01 ± 0.00	0.13 ± 0.27
	Femur	0.43 ± 0.14	1.30 ± 0.58	0.02 ± 0.01	0.02 ± 0.00	0.01 ± 0.00
***C*-NETA**	Blood	1.33 ± 0.32	0.39 ± 0.07	0.05 ± 0.02	0.03 ± 0.01	0.01 ± 0.01
	Liver	2.79 ± 0.24	2.41 ± 0.34	3.19 ± 0.54	4.01 ± 0.53	2.98 ± 0.44
	Spleen	0.63 ± 0.14	0.27 ± 0.05	0.31 ± 0.04	0.20 ± 0.02	0.24 ± 0.02
	Kidney	3.37 ± 0.23	2.21 ± 0.38	2.70 ± 0.26	2.63 ± 0.43	2.18 ± 0.14
	Lung	1.39 ± 0.20	0.69 ± 0.10	0.47 ± 0.09	0.40 ± 0.12	0.31 ± 0.03
	Heart	0.82 ± 0.21	0.51 ± 0.18	0.31 ± 0.02	0.27 ± 0.07	0.25 ± 0.04
	Femur	2.27 ± 0.23	1.79 ± 0.24	1.96 ± 0.28	2.06 ± 0.22	2.31 ± 0.40

Values are the percent injected dose per gram(% ID/g) ± standard deviation